

# Anti-proliferative effect of Fe(III) complexed with 1-(2-hydroxy-3-methoxybenzaldehyde)-4-aminosalicylhydrazone in HepG2 cells

Takeshi Fukushima · Erina Taniguchi · Hiroshi Yamada · Kiyomasa Kato · Ayako Shimizu · Yoshikazu Nishiguchi · Mayu Onozato · Hideaki Ichiba · Yutaro Azuma

Received: 17 February 2015 / Accepted: 25 March 2015  
© Springer Science+Business Media New York 2015

**Abstract** We previously developed a chelating ligand, 1-(2-hydroxy-3-methoxybenzaldehyde)-4-aminosalicylhydrazone (HMB-ASH), which can chelate Fe(III) to form a complex. The HMB-ASH-Fe(III) complex exhibits a dose-dependent anti-proliferative effect in HepG2 cells, whereas the ligand, HMB-ASH, and Fe(III) alone had no considerable effect. The HMB-ASH-Fe(III) complex was composed of Fe(III):HMB-ASH (1:2), as determined by high-performance liquid chromatography with high-resolution mass spectrometry. The IC<sub>50</sub> value was approximately 20 μM, which was comparable to those of the anti-cancer drugs oxaliplatin (OXP) and etoposide (ETP) under

the same conditions. Similar to OXP and ETP, HMB-ASH-Fe(III) induced apoptosis in HepG2 cells, as revealed by terminal deoxynucleotidyl transferase fluorescein-12-dUTP nick end labeling assay.

**Keywords** 1-(2-Hydroxy-3-methoxybenzaldehyde)-4-aminosalicylhydrazone · Metal complex · Anti-proliferation · Fe(III) · HepG2 cells

## Introduction

Cisplatin and oxaliplatin (OXP) are well-known metal complex-containing cancer chemotherapeutics that possess Pt(II) in their structure. In recent studies, a number of metal complexes exhibited anti-proliferative activity in cancer cells in vitro. Recently, numerous organic ligands coordinated with various transition and typical metal ions have been developed, including Pt (Huang et al. 2013), Cu (Farag et al. 2013; Genc et al. 2014), Ni (Genc et al. 2014; Hsu et al. 2013), Fe (Hou and Wang 2005), Zn (Farag et al. 2013; Genc et al. 2014), and Sn (Nath et al. 2014; Mahmudov et al. 2014), which exhibit anti-proliferative activity in cancer cells. These metal complexes could be potential lead compounds for designing novel anticancer drugs.

The reported organic ligands have one or more Schiff base moieties for chelating metal ions. In the Schiff base moiety, the lone pair on the nitrogen atom

**Electronic supplementary material** The online version of this article (doi:10.1007/s10534-015-9852-x) contains supplementary material, which is available to authorized users.

T. Fukushima (✉) · E. Taniguchi · H. Yamada · K. Kato · A. Shimizu · M. Onozato · H. Ichiba  
Department of Analytical Chemistry, Faculty of Pharmaceutical Sciences, Toho University, 2-2-1 Miyama, Funabashi-shi, Chiba 274-8510, Japan  
e-mail: t-fukushima@phar.toho-u.ac.jp

Y. Nishiguchi  
Department of Pharmaceutical Practice, Faculty of Pharmaceutical Sciences, Toho University, 2-2-1 Miyama, Funabashi-shi, Chiba 274-8510, Japan

Y. Azuma  
Department of Medical Biochemistry, Faculty of Pharmaceutical Sciences, Toho University, 2-2-1 Miyama, Funabashi-shi, Chiba 274-8510, Japan

in the azomethine linkage coordinates the metal ions to form a complex. In our laboratory, three organic ligands with Schiff base moieties, 2,4-[bis-(2,4-dihydroxybenzylidene)]-dihydrinoquinazoline (DBHQ) (Kimura et al. 2009a, b), 2,4-[bis-(2-hydroxy-3-methoxybenzylidene)]-dihydrinoquinazoline (HBQZ) (Yamada et al. 2010), and 1-(2-hydroxy-3-methoxybenzaldehyde)-4-aminosalicylhydrazone (HMB-ASH) (Fig. 1) (Yamada et al. 2012), have been developed for the fluorescence detection of Ga(III), Zn(II), and Sc(III), respectively. Additionally, we found that the emitted fluorescence of the HMB-ASH-Sc(III) complex was quenched by adding exogenous Fe(III). These results suggest that a complex of HMB-ASH-Fe(III), which emits no fluorescence, may be formed.

Among the ligand-metal ion combinations we previously developed, the HMB-ASH-Fe(III) complex was chosen for the present study because of its ease synthesis (Yamada et al. 2012) and sufficient stability.

We evaluated the anti-proliferative action of HMB-ASH-Fe(III) in HepG2, K562, and MCF7 cells using the WST-1 assay. Consequently, we found that the HMB-ASH-Fe(III) complex had an intense anti-proliferative effect in HepG2 cells. We further analyzed the chemical structure of the HMB-ASH-Fe(III) complex by ultraviolet (UV) spectroscopy and high-performance liquid chromatography with mass spectrometry (LC-MS). To elucidate whether the HMB-ASH-Fe(III) complex induced apoptosis, DNA fragmentation was examined by TdT-mediated dUDP nick end labeling (TUNEL) assay.

## Materials and methods

### Chemicals

Atomic spectrophotometry-grade  $\text{FeCl}_3$  (1000 ppm in 0.1 N HCl), special grade dimethylsulfoxide (DMSO),

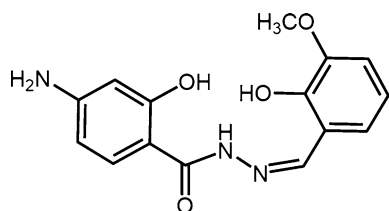


**Fig. 1** Chemical structure of HMB-ASH

HPLC-grade methanol (MeOH), and acetonitrile ( $\text{CH}_3\text{CN}$ ) were obtained from Wako Pure Chemicals (Osaka, Japan). Water was used after purification using a WR600G instrument (Nihon Millipore K.K., Tokyo, Japan). Special-grade ammonium acetate (>97.0 %) was procured from Kanto Chemical Co. Inc. (Tokyo, Japan).

### Synthesis of HMB-ASH

HMB-ASH was synthesized according to our previous paper (Yamada et al. 2012). Briefly, methyl 4-aminosalicylate (4.0 g, 23 mmol) was added to 80 % hydrazine monohydrate (12 mL), and the mixture was refluxed for 90 min. After evaporation, the residue was added to distilled  $\text{H}_2\text{O}$  (20 mL) to obtain a crude crystal. The crude crystal was recrystallized in EtOH to obtain 4-aminosalicylic hydrazide (yield 78.4 %). Subsequently, 4-aminosalicylic hydrazide (0.5 g, 3.0 mmol) in EtOH (100 mL) was reacted with *o*-vanillin (0.45 g, 3.0 mmol) for 2 h in a water bath at 100 °C. After cooling to room temperature, the precipitate was collected by filtration and was recrystallized from MeOH to obtain the final product, HMB-ASH (yield 82.5 %).

FAB-MS:  $m/z$  302 ( $\text{M} + \text{H}$ )<sup>+</sup>; Anal. Calcd. for  $\text{C}_{15}\text{H}_{15}\text{O}_4\text{N}_3$ : C, 59.80; H, 5.02; N, 13.95. Found: C, 60.02; H, 4.89; N, 13.77.  $^1\text{H}$  NMR ( $\text{DMSO}-d_6$ ) (ppm): 12.27 (s, 1H), 11.67 (s, 1H), 11.02 (s, 1H), 8.55 (s, 1H), 7.59 (d, 1H), 7.06 (d, 1H), 6.96 (d, 1H), 6.80 (t, 1H), 6.14 (m, 2H), 6.03 (d, 1H), 5.88 (s, 1H), 3.81 (s, 3H).  $^{13}\text{C}$  NMR ( $\text{DMSO}-d_6$ ) (ppm): 166.31, 162.33, 163.33, 155.25, 148.42, 148.02, 147.63, 129.44, 121.42, 119.46, 114.31, 106.41, 101.88, 99.86, 56.34. FT-IR (solid phase) ( $\text{cm}^{-1}$ ): 3358 ( $\nu_{\text{NH}}$ ), 3236, 1352 ( $\nu_{\text{OH}}$ ), 1599 ( $\nu_{\text{C=N}}$ ), 1250 ( $\nu_{\text{O-CH}_3}$ ). Melting point: 252–254 °C.

### Preparation of HMB-ASH-Fe(III) complex

Forty microliters of 24 mM HMB-ASH in DMSO was mixed with 16 mM  $\text{FeCl}_3$  (60  $\mu\text{L}$ ) in  $\text{H}_2\text{O}$  and 100 mM  $\text{NH}_3\text{-NH}_4\text{Cl}$  buffer (1013  $\mu\text{L}$ ; pH 7.4). The mixed solution was incubated for 10 min at room temperature after mixing with vortex. Subsequently, 0.1 NaOH (87  $\mu\text{L}$ ) was added to prepare 800  $\mu\text{M}$  HMB-ASH-Fe(III) complex. The solution was then diluted with culture medium, as described below, to prepare 12.5, 25, 50, 100, and 200  $\mu\text{M}$  HMB-ASH-Fe(III) complex solution. For the blanks without

HMB-ASH or Fe(III), DMSO (40  $\mu\text{L}$ ) or  $\text{H}_2\text{O}$  (60  $\mu\text{L}$ ) was added to prepare the solution.

#### Cell culture and anti-proliferation assay

Human hepatocellular carcinoma HepG2 cells and human breast cancer MCF7 cells (JCRB Cell Bank, National Institute of Biomedical Innovation, Osaka, Japan) were cultured in Dulbecco's modified Eagle's medium [Nissui Pharmaceutical Co., Ltd. (Tokyo, Japan)] supplemented with 10 % fetal bovine serum (FBS), and human leukemia K562 cells (JCRB Cell Bank) were cultured in RPMI-1640 medium [Nissui Pharmaceutical Co., Ltd. (Tokyo, Japan)] supplemented with 10 % FBS [Nissui Pharmaceutical Co., Ltd. (Tokyo, Japan)]. The anti-proliferative effect of the complexes was assayed in 96-well microplates using WST-1 reagent (Dojindo Laboratories Co., Ltd., Kumamoto, Japan). Briefly, HepG2 and MCF7 cells ( $1.0 \times 10^5$  cells/mL) were suspended and seeded into 96-well plates at a density of  $5.0 \times 10^3$  cells/well/50  $\mu\text{L}$ . K562 cells were also suspended ( $2.0 \times 10^5$  cells/mL) and seeded at a density of  $1.0 \times 10^4$  cells/well/50  $\mu\text{L}$ . The cells were pre-incubated at 37 °C for 24 h in a humidified atmosphere containing 5 %  $\text{CO}_2$ . Subsequently, 50  $\mu\text{L}$  of the complex solution (12.5, 25, 50, 100, or 200  $\mu\text{M}$ ) was added to each well and incubated for 48 h ( $n = 3$ ).

After incubation for 48 h, 10  $\mu\text{L}$  of WST-1 reagent was added and incubated for 2 h. The absorbance at 450 nm was measured and analyzed using a Beckman Coulter DTX 800 Multimode Detector plate reader (Beckman Coulter, Brea, CA, USA). The obtained data were expressed as mean  $\pm$  standard error (S.E.) ( $n = 3$ ).

#### UV spectra of HMB-ASH-Fe(III) complex

Five milliliters of HMB-ASH in DMSO (1.0 mM) was diluted with methanol in a volumetric flask (50 mL) to prepare a 100  $\mu\text{M}$  solution. The HMB-ASH solution (1.0 mL) was mixed with 0.90–90  $\mu\text{M}$  Fe(III) solution (0.1–2.0 mL) and 100 mM ammonia-buffered solution (1.0 mL, pH 8.0), and incubated for 10 min at room temperature. The mixed solution was diluted to 5.0 mL with methanol by volumetric flask. The combined solution was manually mixed, and was

subjected to UV spectrometry by JASCO V-650 (Jasco, Tokyo, Japan).

#### LC-atmospheric pressure chemical ionization (APCI)-MS

HMB-ASH (100  $\mu\text{M}$ , 200  $\mu\text{L}$ ) was mixed with 200  $\mu\text{M}$  Fe(III) solution (100  $\mu\text{L}$ ) and 10 %  $\text{CH}_3\text{CN}$ -100 mM ammonia-buffered solution (pH 8.0, 700  $\mu\text{L}$ ), and the solution was mixed vigorously for 15 s. The solution (50  $\mu\text{L}$ ) was injected through an autosampler onto an LC-time-of-flight (TOF)-MS system, comprising an Agilent 1200 series HPLC system (Agilent Technologies, Santa Clara, CA, USA) and a TOF-MS (JMS-T100 LP AccuTOF LC-Plus) equipped with an atmospheric pressure chemical ionization (APCI) source (JEOL Co. Ltd., Tokyo, Japan). The separation column was a CAPCELL PAK C18 MG-II (100 mm  $\times$  4.6 mm; i.d.: 3  $\mu\text{m}$ ; Shiseido Co., Ltd., Tokyo, Japan), and the mobile phase was 5.0 mM  $\text{CH}_3\text{CO}_2\text{NH}_4$  in  $\text{H}_2\text{O}:\text{CH}_3\text{CN}$  (90:10) (A) and  $\text{CH}_3\text{CN}$  (B). The mobile phase was eluted by a linear gradient program; 0 min A/B = 70/30, 12.0 min A/B = 42/58, 12.1 min A/B = 42/58, 22.0 min A/B = 42/58, 22.1 min A/B = 70/30, and 32 min A/B = 70/30. The flow rate was constant at 0.8 mL  $\text{min}^{-1}$ , and the column temperature was maintained at 35 °C. The APCI-MS conditions were as follows: negative ion mode; needle voltage set at  $-4501$  V; and the ring lens and orifice 1 and 2 voltages set at  $-20$ ,  $-80$ , and  $-15$  V, respectively. Nitrogen was used as the nebulizing and desolvation gas, and the pressure was maintained constant at 0.608 MPa. The desolvation chamber and orifice 1 temperatures were set to 420 and 80 °C, respectively. Simultaneously, UV detection was carried out at 335 nm. Data were obtained using Mass Center software, MS-56010MP (JEOL).

#### DNA fragmentation

DNA fragmentation was assessed using the Dead-End<sup>TM</sup> Fluorometric TUNEL System (Promega KK, Tokyo, Japan). Briefly, HepG2 cells were seeded ( $1.0 \times 10^5$  cells/well) in 4-well glass plates, and were pre-incubated for 24 h. Subsequently, 100  $\mu\text{M}$  HMB-ASH (50  $\mu\text{L}$ ) in the presence or absence of Fe(III) or 100  $\mu\text{M}$  OXP or etoposide (ETP) was added and incubated for 24 h. After the incubation, the cells were washed with 200  $\mu\text{L}$  of PBS, and then treated with 4 %

formaldehyde solution (200  $\mu\text{L}$ ). The treated cells were placed on ice for 25 min. Subsequently, the cells were washed twice with 200  $\mu\text{L}$  of PBS and treated with 0.1 % Triton<sup>®</sup> X-100 (100  $\mu\text{L}$ ) for 5 min at room temperature. After washing with 200  $\mu\text{L}$  of PBS, the cells were incubated for 5 min, and mixed with 50  $\mu\text{L}$  of equilibration buffer containing the nucleotide mix (fluorescein-12-dUTP) and recombinant terminal deoxynucleotidyl transferase (rTdT). The cells were incubated at 37 °C for 60 min. Subsequently, 500  $\mu\text{L}$  of saline sodium citrate buffer (SSC, 20 $\times$ ) diluted tenfold with H<sub>2</sub>O was added, and samples were incubated for 15 min to stop the enzyme reaction. After washing twice with 200  $\mu\text{L}$  of PBS, apoptotic cells were examined by confocal fluorescence microscopy. The stained cells were scanned using the confocal laser scanning microscope, LSM 510 Meta (Carl Zeiss, Oberkochen, Germany, ex. 488 nm, 40  $\times$  water-immersion objective lens).

#### Flow cytometry

As described above, HMB-ASH-Fe(III) complex, OXP, and ETP were added to HepG2 cells and incubated for 24 h. After incubation, cells were washed with 2 mL of PBS, followed by incubation for 5 min at room temperature. Subsequently, the cells were detached by adding 0.02 % EDTA in PBS (100  $\mu\text{L}$ ), followed by incubation at 37 °C for 15 min. The collected cells were centrifuged at 1000 *g* for 3 min at 4 °C, and the supernatant was removed. The pelleted cells were treated with 1 % formaldehyde solution (100  $\mu\text{L}$ ) and were incubated for 20 min on ice. After centrifugation at 1000 *g* for 3 min at 4 °C, the supernatant was removed. The pelleted cells were treated with 0.1 % Triton<sup>®</sup> X-100 (50  $\mu\text{L}$ ), and were incubated for 5 min on ice. The cells were suspended in 1 mL of PBS and centrifuged at 1000 *g* for 3 min at 4 °C. After removing the supernatant, equilibration buffer (100  $\mu\text{L}$ ) was added and incubated for 60 min at 37 °C. EDTA (20 mM, 1 mL) was added and vortexed to stop the reaction. After centrifugation, the pelleted cells were resuspended in 100  $\mu\text{L}$  of PBS. The resultant cells were mixed with 1 mL of BD FACSFlow Sheath Fluid (BD Biosciences, San Jose, CA, USA) and analyzed by a flow cytometer. Two-color flow cytometric analysis was performed using a FACS Calibur flow cytometer (BD Biosciences). Analysis was done using FlowJo software (Tree Star, Ashland, OR, USA).

## Results

### Anti-proliferative action of the HMB-ASH-Fe(III) complex

We first examined the anti-proliferative action of the HMB-ASH-Fe(III) complexes on HepG2 cells, as compared to HMB-ASH or Fe(III) alone using a WST-1 assay. As shown in Fig. 2, HMB-ASH or Fe(III) alone had no effect on the HepG2 cells (Fig. 2a, b). In contrast, HMB-ASH-Fe(III) exhibited a dose-dependent anti-proliferative effect in HepG2 cells (Fig. 2c). Interestingly, the anti-proliferative effect of the HMB-ASH-Fe(III) complexes was remarkable high in HepG2 cells, whereas slight inhibition was observed in MCF7 and K562 cells (Fig. 3a). These results suggest that HMB-ASH-Fe(III) complexes are remarkably potent growth inhibitors in HepG2 cells. The IC<sub>50</sub> value was approximately 20  $\mu\text{M}$ . The anti-proliferative effect of the HMB-ASH-Fe(III) complexes was more potent than the traditional chemotherapy, and was similar to OXP under the present experimental conditions (Fig. 3b). Thus, HMB-ASH-Fe(III) complexes may have similar anti-proliferative potency to ETP and OXP in HepG2 cells.

### UV spectra of HMB-ASH-Fe(III) complex

Although our previous work suggested HMB-ASH binds Fe(III) (Yamada et al. 2012), the chemical structure of the HMB-ASH-Fe(III) complex was unknown. To better understand the chemical structure of the HMB-ASH-Fe(III) complex, the binding ratio of HMB-ASH to Fe(III) was evaluated by UV titration. Figure 4a shows the changes in the HMB-ASH UV spectra as a function of Fe(III) concentration. As the Fe(III) concentration increased, the UV spectra changed, with an isosbestic point at 364 nm, suggesting that HMB-ASH bound Fe(III) to form a complex. Below 364 nm, the absorbance decreased with an increase in Fe(III) concentration. In contrast, the absorbance was increased above 364 nm. Using the absorbance at 460 nm, a molar ratio plot (Fig. 4b) was drawn, because it prevented the absorbance of Fe(III) itself. The molar ratio plot indicated that HMB-ASH can bind to Fe(III) at a molar ratio of 2:1. In addition, the apparent binding constant *K*, calculated by Benesi-Hildebrand plot (Roy et al. 2007), was  $3.06 \times 10^7$ , based on the absorbance changes at 460 nm.

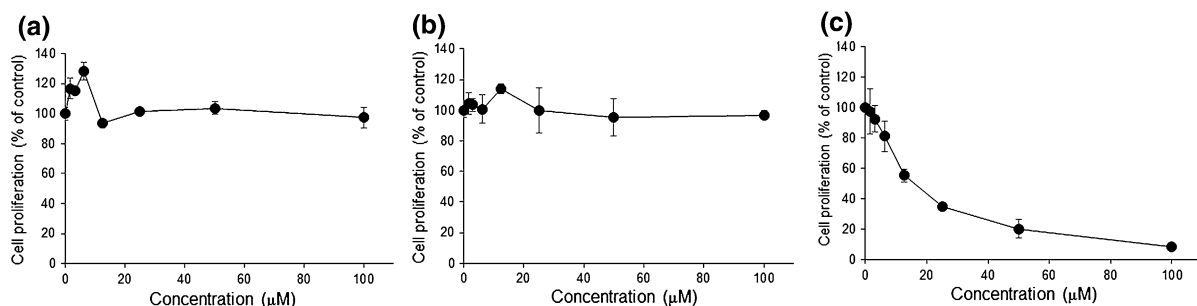


**Fig. 2** Anti-proliferative effects of HMB-ASH (a), Fe(III) (b), and the HMB-ASH-Fe(III) complexes (c) in HepG2 cells (closed circle with solid line). [mean  $\pm$  S.E. ( $n = 3$ )]

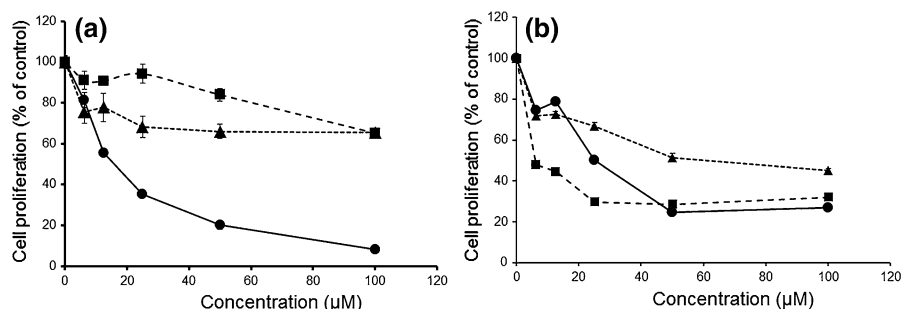
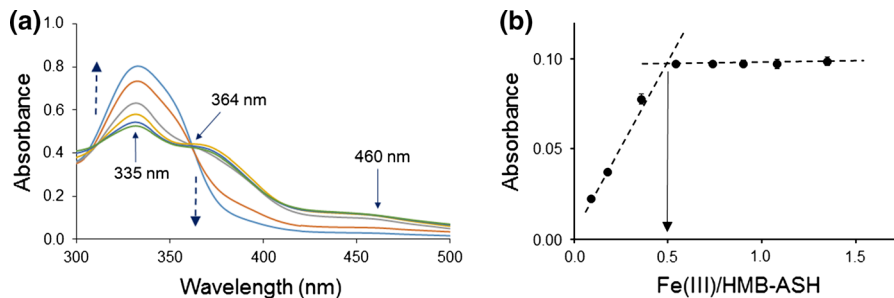


**Fig. 3** (a) Anti-proliferative effects of the HMB-ASH-Fe(III) complexes on HepG2 (closed circle with solid line), MCF7 (closed square with dotted line), and K562 cells (closed triangle with dashed line). [mean  $\pm$  S.E. ( $n = 3$ )], and (b) Anti-

proliferative effects of the HMB-ASH-Fe(III) complexes (closed circle with solid line), oxaliplatin (closed square with dashed line), and etoposide (closed triangle with dotted line) in HepG2 cells. [mean  $\pm$  S.E. ( $n = 3$ )]

**Fig. 4** UV-Vis spectrum of HMB-ASH with Fe(III) (a) and molar ratio plot at 460 nm (b). Dashed arrow in (a) indicates an increase in Fe(III) concentration (100, 200, 400, 600, 800, and 1000  $\mu$ M)



#### Chromatographic and accurate mass analysis by LC-TOF-MS

Figure 5 shows representative chromatograms for HMB-ASH (Fig. 5a) and HMB-ASH mixed with Fe(III) (Fig. 5b), obtained by reversed-phase HPLC with UV detection at 335 nm. HMB-ASH itself eluted at approximately 4 min. However, after adding Fe(III), HMB-ASH peak at 4 min completely disappeared. Rather, a new peak eluted at 8.6 min. The peak

at approximately 8.6 min may be the HMB-ASH-Fe(III) complex, because it may have an increased hydrophobicity as compared to HMB-ASH. As determined by LC-TOF-MS analysis, the peak at 8.6 min was a peak of HMB-ASH-Fe(III) complex, of which the  $m/z$  was 654.11620 (Fig. 6a), indicating that the elemental composition of HMB-ASH-Fe(III) was  $C_{30}H_{26}O_8N_6Fe$  (error  $-1.17$  ppm). From these accurate mass data, the presumed structure of the HMB-ASH-Fe(III) complex was two molecules of

**Fig. 5** Chromatograms of HMB-ASH (a) and the HMB-ASH-Fe(III) complexes (b), obtained by reversed-phase HPLC with UV detection (335 nm). Experimental details are described in the text

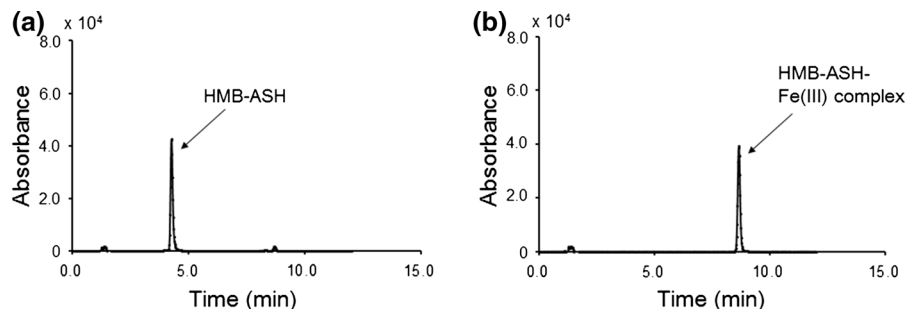
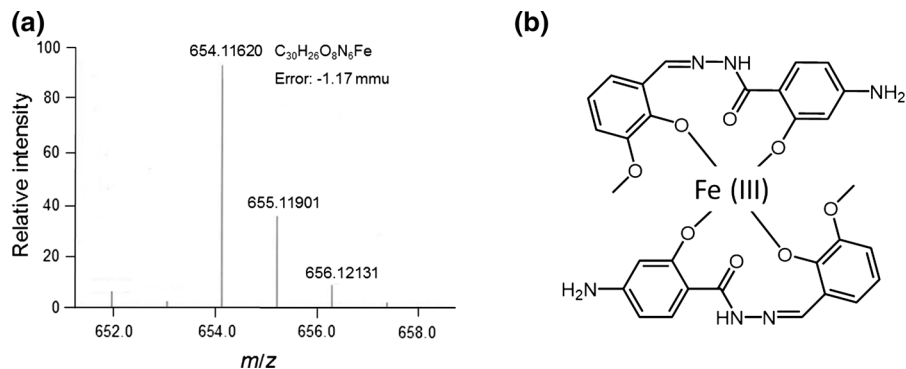


**Fig. 6** Mass spectrum of the HMB-ASH-Fe(III) complexes obtained by LC-TOF-MS (a) and the presumed chemical structure of HMB-ASH-Fe(III) complexes (b)



HMB-ASH bound to Fe(III), with deletion of four protons in 2 HMB-ASH ( $[2\text{HMB-ASH} + \text{Fe(III)} - 4\text{H}]^-$ ) (Fig. 6b).

#### DNA fragmentation and flow cytometry

Using confocal fluorescence microscopy, fluorescein-12-dUTP fluorescence spots (TUNEL-positive cells) were clearly observed in cells treated with HMB-ASH-Fe(III) complexes, as well as those treated with OXP and ETP (Fig. 7c, d, e). In contrast, few fluorescence spots were observed in HepG2 cells treated with HMB-ASH without Fe(III) (Fig. 7b). These results were in agreement with the data in Fig. 2, in which HMB-ASH-Fe(III) complex, but not HMB-ASH alone, exhibited anti-proliferative effects.

To further confirm apoptosis in HepG2 cells, a flow cytometric analysis was carried out. As shown in Fig. 8a, HMB-ASH-Fe(III) complex-induced DNA fragmentation may occur because the HMB-ASH-Fe(III) complex exhibits similar shifts to OXP, as compared with the control. The area of fluorescence in the TUNEL-positive cells after HMB-ASH-Fe(III) complex treatment was nearly similar to that of OXP (Fig. 8b).

#### Discussion

The purpose of this study was to elucidate the anti-proliferative effect of metal complexes comprised of a Schiff-base in cell lines in vitro using HMB-ASH, a previously developed compound. The anti-proliferative effect of the HMB-ASH-Fe(III) complex was relatively weak in a human breast cancer cell lines (MCF-7 cells) and chronic myelogenous leukemia cell line (K562 cells); however, the human liver carcinoma cell line, HepG2, was significantly inhibited by HMB-ASH-Fe(III) complexes. Therefore, HMB-ASH-Fe(III) complexes may have selective and pronounced activity against HepG2 cells. To date, several metal complexes containing Co(II), Ni(II), Zn(II), Pt(II), Ru(II), Sn(II), or Cu(II) have shown anti-proliferative effects in HepG2 cells (Alexandrova et al. 2012; Chen et al. 2013; Dyakova et al. 2014; Farag et al. 2013; Mahmudov et al. 2014; Rubino et al. 2014; Tan et al. 2009; Thati et al. 2007). This is the first report of HepG2 cell growth inhibition using complexes chelating the transition metal, Fe(III). Generally, iron is one of the most important elements for cellular proliferation. Thus, complex formation between iron-depleting agents

**Fig. 7** Apoptosis detection using the TUNEL assay in HepG2 cells treated with control (a), HMB-ASH (b), HMB-ASH-Fe(III) complexes (c), oxaliplatin (d), and etoposide (e) after 24 h, as viewed under laser scanning confocal microscopy. Magnification at  $60 \times 10$

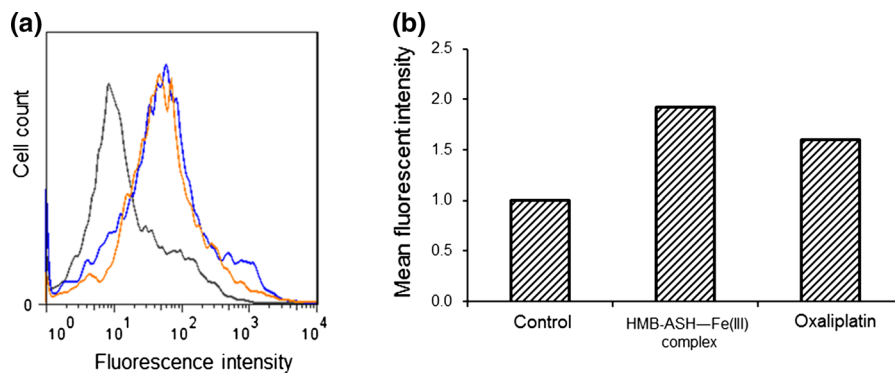
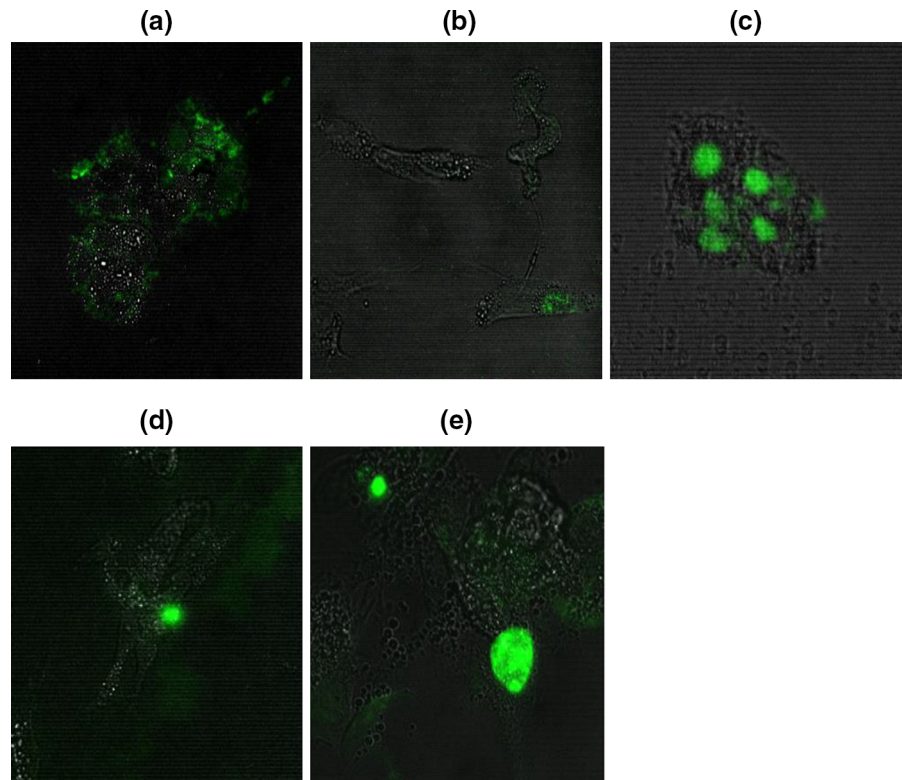


**Fig. 8** Flow cytometric analysis of HepG2 cells treated with control (medium, *black*), HMB-ASH-Fe(III) complex (*blue*), and oxaliplatin (*orange*) (a), and the integrated fluorescence intensity (b). (Color figure online)

and Fe(III) in cells can induce apoptosis (Yu et al. 2012). To date, several iron chelators, such as desferrioxamine (Desferal<sup>®</sup>), 5-hydroxypyridine-2-carboxaldehyde thiosemicarbazone, and pyridoxal isonicotinoyl hydrazone, could serve as anti-cancer drugs for refractory leukemia, gastrointestinal tumor, and children with neuroblastoma etc. (Kovacevic et al. 2011; Yu et al. 2012). These compounds have

chelation sites in their structures to capture Fe(II) or Fe(III) in cancer cells. HMB-ASH can also chelate Fe(III) with a binding constant of  $10^7$ . Thus, it is hypothesized that HMB-ASH may act as an iron chelator in HepG2 cells. However, HMB-ASH itself has no anti-proliferative effect, suggesting that the complex of HMB-ASH and Fe(III) is crucial for the anti-proliferative effect on HepG2 cells. When

prepared using the batch method, the HMB–ASH–Fe(III) complex is relatively stable, due to the binding constant that is  $10^7$  order of HMB–ASH to Fe(III) in weak basic pH. In addition, a clear single peak for HMB–ASH–Fe(III) was observed using reversed-phase chromatography with a mobile phase of 5.0 mM ammonium acetate solution (pH 7.0). Given the high stability under neutral to weak basic pH conditions, it seems unlikely that the HMB–ASH–Fe(III) complex dissociated completely in cells. Therefore, it is likely that the anti-proliferative effect of the HMB–ASH–Fe(III) complex differs from the mechanism of other iron-deprived chelators.

The anti-proliferative effect of the HMB–ASH–Fe(III) complexes is likely related to DNA fragmentation, as was clearly observed using the TUNEL assay. This was similar to other anticancer drugs, including OXP and ETP. Based on these results, the HMB–ASH–Fe(III) complex induces apoptosis in HepG2 cells.

In the present study, we failed to elucidate the three-dimensional structure of the HMB–ASH–Fe(III) complex by X-ray crystallography. We tried a preliminary extraction of the HMB–ASH–Fe(III) complex using liquid–liquid extraction with  $\text{CH}_2\text{Cl}_2$  to obtain a single crystal; however, the extract was a black powder, and not a single crystal. As shown in Fig. S1, the powder also exhibited anti-proliferative activity in HepG2 cells, indicating that the powder contains the HMB–ASH–Fe(III) complex. The powder had an identical UV and mass spectra to those in Figs. 4a and 6a; however, a single crystal of the HMB–ASH–Fe(III) complex could not be obtained by recrystallization. Therefore, structural X-ray analysis was not performed. Although the HMB–ASH–Fe(III) complex was assumed, as shown in Fig. 6 b, by LC–TOF–MS analysis and UV absorption spectrometry, three-dimensional analysis on the HMB–ASH–Fe(III) complex is requisite in the future.

We showed that HMB–ASH–Fe(III) complexes have an anti-proliferative effect specifically in HepG2 cells via the induction of apoptosis, and that this effect was comparable to that of ETP and OXP in HepG2 cells. In order to develop HMB–ASH–Fe(III) complexes as a novel anti-proliferative compound, further work is necessary to clarify the detailed mechanism of action elucidate the structure by X-ray crystallography.

**Acknowledgments** The authors thank Drs. Iwasa and Iizuka, Toho University for their valuable discussions on this study, and

Mr. T. Abe, T. Sakamoto, and Miss M. Hanaoka for their technical assistance.

## References

- Alexandrova RI, Zhivkova T, Alexandrov M, Miloshev G, Georgieva M, Pantcheva IN, Mitewa MI (2012) Cytostatic and cytotoxic properties of monensic acid and its biometal(II) complexes against human tumor/non-tumor cell lines. *Cent Eur J Chem* 10:1464–1474. doi:[10.2478/s11532-012-0071-9](https://doi.org/10.2478/s11532-012-0071-9)
- Chen Y, Qin MY, Wang L, Chao H, Ji LN, Xu AL (2013) A ruthenium(II) beta-carboline complex induced p53-mediated apoptosis in cancer cells. *Biochimie* 95:2050–2059. doi:[10.1016/j.biochi.2013.07.016](https://doi.org/10.1016/j.biochi.2013.07.016)
- Dyakova L, Culita DC, Marinescu G, Alexandrov M, Kalfin R, Patron L, Alexandrova R (2014) Metal Zn(II), Cu(II), Ni(II) complexes of ursodeoxycholic acid as putative anticancer agents. *Biotechnol Biotechnol Equip* 28:543–551. doi:[10.1080/13102818.2014.927973](https://doi.org/10.1080/13102818.2014.927973)
- Farag AM, Guan TS, Osman H, Majid A, Iqbal MA, Ahamed MBK (2013) Synthesis of metal(II) M = Cu, Mn, Zn Schiff base complexes and their Pro-apoptotic activity in liver tumor cells via caspase activation. *Med Chem Res* 22:4727–4736. doi:[10.1007/s00044-013-0482-y](https://doi.org/10.1007/s00044-013-0482-y)
- Genc Z, Selcuk S, Sandal S, Colak N, Keser S, Sekerci M, Karatepe M (2014) Spectroscopic, antiproliferative and antiradical properties of Cu(II), Ni(II), and Zn(II) complexes with amino acid based Schiff bases. *Med Chem Res* 23:2476–2485. doi:[10.1007/s00044-013-0826-7](https://doi.org/10.1007/s00044-013-0826-7)
- Hou MH, Wang AHJ (2005) Mithramycin forms a stable dimeric complex by chelating with Fe(II): dNA-interacting characteristics, cellular permeation and cytotoxicity. *Nucleic Acids Res* 33:1352–1361. doi:[10.1093/nar/gki276](https://doi.org/10.1093/nar/gki276)
- Hsu C, Kuo C, Chuang S, Hou M (2013) Elucidation of the DNA-interacting properties and anticancer activity of a Ni(II)-coordinated mithramycin dimer complex. *Biometals* 26:1–12. doi:[10.1007/s10534-012-9589-8](https://doi.org/10.1007/s10534-012-9589-8)
- Huang KB, Chen ZF, Liu YC, Li ZQ, Wei JH, Wang M, Zhang GH, Liang H (2013) Platinum(II) complexes with mono-aminophosphonate ester targeting group that induce apoptosis through G1 cell-cycle arrest: synthesis, crystal structure and antitumour activity. *Eur J Med Chem* 63:76–84. doi:[10.1016/j.ejmech.2013.01.055](https://doi.org/10.1016/j.ejmech.2013.01.055)
- Kimura J, Yamada H, Ogura H, Yajima T, Fukushima T (2009a) Development of a fluorescent chelating ligand for gallium ion having a quinazoline structure with two Schiff base moieties. *Anal Chim Acta* 635:207–213. doi:[10.1016/j.aca.2009.01.008](https://doi.org/10.1016/j.aca.2009.01.008)
- Kimura J, Yamada H, Yajima T, Fukushima T (2009b) Enhancement effect of some phosphorylated compounds on fluorescence of quinazoline-based chelating ligand complexed with gallium ion. *J Lumin* 129:1362–1365. doi:[10.1016/j.jlumin.2009.07.005](https://doi.org/10.1016/j.jlumin.2009.07.005)
- Kovacevic Z, Kalinowski DS, Lovejoy DB, Yu Y, Rahmanto YS, Sharpe PC, Bernhardt PV, Richardson DR (2011) The medicinal chemistry of novel iron chelators for the treatment of cancer. *Curr Top Med Chem* 11:483–499. doi:[10.2174/156802611794785190](https://doi.org/10.2174/156802611794785190)

- Mahmudov KT, da Silva M, Kopylovich MN, Fernandes AR, Silva A, Mizar A, Pombeiro AJL (2014) Di- and triorganotin(IV) complexes of arylhydrazones of methylene active compounds and their antiproliferative activity. *J Organomet Chem* 760:67–73. doi:[10.1016/j.jorganchem.2013.12.019](https://doi.org/10.1016/j.jorganchem.2013.12.019)
- Nath M, Vats M, Roy P (2014) Design, spectral characterization, anti-tumor and anti-inflammatory activity of triorganotin(IV) hydroxycarboxylates, apoptosis inducers: in vitro assessment of induction of apoptosis by enzyme, DNA-fragmentation, acridine orange and comet assays. *Inorg Chim Acta* 423:70–82. doi:[10.1016/j.ica.2014.02.034](https://doi.org/10.1016/j.ica.2014.02.034)
- Roy P, Dhara K, Manassero M, Ratha J, Banerjee P (2007) Selective fluorescence zinc ion sensing and binding behavior of 4-methyl-2,6-bis(((phenylmethyl)imino)methyl)phenol: biological application. *Inorg Chem* 46:6405–6412. doi:[10.1021/ic700420w](https://doi.org/10.1021/ic700420w)
- Rubino S, Di Stefano V, Attanzio A, Tesoriere L, Girasolo MA, Nicolo F, Bruno G, Orecchio S, Stocco GC (2014) Synthesis, spectroscopic characterization and antiproliferative activity of two platinum(II) complexes containing N-donor heterocycles. *Inorg Chim Acta* 418:112–118. doi:[10.1016/j.ica.2014.03.028](https://doi.org/10.1016/j.ica.2014.03.028)
- Tan J, Wang BC, Zhu LC (2009) DNA binding, cytotoxicity, apoptotic inducing activity, and molecular modeling study of quercetin zinc(II) complex. *Bioorganic Med Chem* 17:614–620. doi:[10.1016/j.bmc.2008.11.063](https://doi.org/10.1016/j.bmc.2008.11.063)
- Thati B, Noble A, Creaven BS, Walsh M, Kavanagh K, Egan DA (2007) Apoptotic cell death: a possible key event in mediating the in vitro anti-proliferative effect of a novel copper(II) complex, Cu(4-Mecdoa) (phen)(2) (phen = phenanthroline, 4-Mecdoa = 4-methylcoumarin-6, 7-dioxactetate), in human malignant cancer cells. *Eur J Pharmacol* 569:16–28. doi:[10.1016/j.ejphar.2007.04.064](https://doi.org/10.1016/j.ejphar.2007.04.064)
- Yamada H, Shirai A, Kato K, Kimura J, Ichiba H, Yajima T, Fukushima T (2010) Development of a quinazoline-based chelating ligand for zinc ion and its application to validation of a zinc-Ion-coordinated compound. *Chem Pharm Bull* 58:875–878
- Yamada H, Kojo M, Nakahara T, Murakami K, Kakima T, Ichiba H, Yajima T, Fukushima T (2012) Development of a fluorescent chelating ligand for scandium ion having a Schiff base moiety. *Spectrochim Acta Part A* 90:72–77. doi:[10.1016/j.saa.2012.01.014](https://doi.org/10.1016/j.saa.2012.01.014)
- Yu Y, Gutierrez E, Kovacevic Z, Saletta F, Obeidy P, Rahmanto YS, Richardson DR (2012) Iron chelators for the treatment of cancer. *Curr Med Chem* 19:2689–2702